HHS Public Access

Author manuscript

Oncogene. Author manuscript; available in PMC 2012 January 28.

Published in final edited form as:

Oncogene. 2011 July 28; 30(30): 3370–3380. doi:10.1038/onc.2011.51.

A Novel Small Molecule Antagonist of Choline Kinase-α That Simultaneously Suppresses MAPK and PI3K/AKT Signaling

Brian F. Clem[1,2,3], **Amy L. Clem**[1,3], **Abdullah Yalcin**[1,2,3,5], **Umesh Goswami**[1,3], **Sengodagounder Arumugam**[4], **Sucheta Telang**[1,2,3], **John O. Trent**[1,2,3,4,#], and **Jason Chesney**[1,2,3,*]

[1]Department of Medicine, University of Louisville, Louisville, KY

[2]Department of Biochemistry and Molecular Biology, University of Louisville, Louisville, KY

[3]Department of Molecular Targets Group, University of Louisville, Louisville, KY

[4]Structural Biology Program James Graham Brown Cancer Center, University of Louisville, Louisville, KY

[5]Department of Biochemistry, School of Veterinary Medicine, Uludag University, Bursa, Turkey

Abstract

Choline kinase-α expression and activity are increased in multiple human neoplasms as a result of growth factor stimulation and activation of cancer-related signaling pathways. The product of choline kinase-α, phosphocholine, serves as an essential metabolic reservoir for the production of phosphatidylcholine, the major phospholipid constituent of membranes and substrate for the production of lipid second messengers. Using *in silico* screening for small molecules that may interact with the choline kinase-α substrate binding domain, we identified a novel competitive inhibitor, N-(3,5-dimethylphenyl)-2-[[5-(4-ethylphenyl)-1H-1,2,4-triazol-3-yl]sulfanyl] acetamide (*termed* CK37) that inhibited purified recombinant human choline kinase-α activity, reduced the steady-state concentration of phosphocholine in transformed cells, and selectively suppressed the growth of neoplastic cells relative to normal epithelial cells. Choline kinase-α activity is required for the downstream production of phosphatidic acid, a promoter of several Ras signaling pathways. CK37 suppressed MAPK and PI3K/AKT signaling, disrupted actin cytoskeletal organization, and reduced plasma membrane ruffling. Finally, administration of CK37 significantly decreased tumor growth in a lung tumor xenograft mouse model, suppressed tumor phosphocholine, and diminished activating phosphorylations of ERK and AKT *in vivo*. Together, these results further validate choline kinase-α as a molecular target for the development of agents that interrupt Ras signaling pathways, and indicate that receptor-based computational screening should facilitate the identification of new classes of choline kinase-α inhibitors.

[*] Corresponding author for entire study: 505 S. Hancock St., CTRB, Rm. 424, University of Louisville, Louisville, KY 40202.
[#]Corresponding author for *in silico* screen (Fig. 1a): 505 S. Hancock St., CTRB, Rm. 224, University of Louisville, Louisville, KY 40202

Conflict of Interest: BFC, ST, JOT, and JC are listed as inventors on a submitted patent concerning content within this manuscript. The University of Louisville is the recognized patent holder.

Keywords

Chemotherapy; Choline Kinase; Metabolism; *In silico*; Phosphocholine

Introduction

Evidence for the requirement of choline kinase-α activity in cancer has been obtained from observations that choline kinase-α expression is elevated in many tumor types and that this increase correlates with poor prognosis in both lung and breast cancer patients (Iorio *et al.*, 2005; Ramirez de Molina *et al.*, 2002a; Ramirez de Molina *et al.*, 2002c). siRNA silencing of choline kinase-α mRNA expression reduces intracellular phosphocholine, which in turn decreases cellular proliferation and promotes differentiation in MDA-MB-231 breast cancer cells (Glunde *et al.*, 2005). Furthermore, pro-oncogenic stimuli, including insulin, platelet-derived growth factor, fibroblast growth factor, epidermal growth factor, prolactin, estrogens and hypoxia-inducible factor-1α, each have been found to stimulate choline kinase-α activity and increase intracellular phosphocholine (Chung *et al.*, 2000; Glunde *et al.*, 2008; Jimenez *et al.*, 1995; Ko *et al.*, 1986; Neeman and Degani, 1989; Uchida, 1996; Warden and Friedkin, 1985).

Choline kinase executes the first committed step within the cytidyl diphosphocholine (Kennedy) pathway, which allows for the production of the major membrane lipid component phosphatidylcholine (PC). The phospholipase D mediated catabolism of PC yields diacylglycerol and phosphatidic acid, which each have been shown to be significant lipid second messengers involved in several signaling pathways (Exton, 1990; Hancock, 2007; Rizzo and Romero, 2002). Phosphatidic acid binds to the amino-terminal Pleckstrin homology domain of the Ras specific guanine-nucleotide exchange factor Sos with high affinity and specificity and promotes the recruitment of Sos to the plasma membrane (Zhao *et al.*, 2007). Phosphatidic acid also binds to Raf-1 via a 36 amino acid region within the kinase domain and promotes its recruitment to the plasma membrane where it is activated by direct interaction with Ras (Rizzo *et al.*, 1999; Rizzo *et al.*, 2000; Scales and Scheller, 1999; Zhao *et al.*, 2007). Accordingly, phosphatidylcholine-derived phosphatidic acid functions in part as a mediator of the Ras signaling pathway and thus the choline kinase metabolite phosphocholine may be essential for the amplification of growth factor signaling cascades required for survival and growth. We recently demonstrated that siRNA-mediated inhibition of choline kinase-α suppressed both MAPK and AKT signaling, and that the addition of phosphatidic acid rescued ERK1/2 activation (Yalcin *et al.*, 2009). In independent studies, Chua *et al.* also established that choline kinase-α is required for the activation of AKT in breast carcinoma cells (Chua *et al.*, 2009). Taken together, these studies indicate that choline kinase-α activity may be essential for tumor progression not only for the production of essential phospholipids required for membrane synthesis, but also for the activation of downstream oncogenic signaling pathways.

Hemicholinium-3 (HC-3) is a known competitive inhibitor of choline kinase that has structural homology to choline. HC-3 and several of its derivatives have been found to inhibit cancer cell proliferation (Hernandez-Alcoceba *et al.*, 1999; Hernandez-Alcoceba *et*

al., 1997; Rodriguez-Gonzalez *et al.*, 2003). One HC-3 derivative in particular, termed MN58b, inhibits endogenous choline kinase activity and suppresses breast cancer, colon cancer, and epidermoid carcinoma xenograft growth *in vivo* (Hernandez-Alcoceba *et al.*, 1999; Hernandez-Alcoceba *et al.*, 1997; Ramirez de Molina *et al.*, 2004a; Rodriguez-Gonzalez *et al.*, 2003). The pre-clinical activities of HC-3 derivatives against xenografts coupled to the recently identified requirement of choline kinase for MAPK and AKT signaling provide substantial rationale for efforts to discover new classes of choline kinase antagonists.

Herein, we report the *in silico* identification and biological verification of a novel small molecule inhibitor of choline kinase-α that suppresses survival signaling and tumorigenic growth in mice. Our data support the targeting of choline kinase-α as an approach for the development of therapeutics for cancers that rely on Ras signaling, and demonstrate the utility of computational screening as a valid means of identifying novel choline kinase-α inhibitors.

Results

Computational Screening for Small Molecule Inhibitors of Choline Kinase-α

We used the recently described X-ray structure of human choline kinase-α (Malito *et al.*, 2006) to conduct an *in silico* screen of the ZINC Library to identify potential choline kinase-α interacting compounds. Fifty compounds were identified, scored, ranked, and analyzed based on their association potential with the active site within choline kinase-α. We physically tested the 16 best-score compounds for their ability to inhibit choline kinase-α activity in HeLa cell lysates. Only one of the screened compounds, N-(3,5-dimethylphenyl)-2-[[5-(4-ethylphenyl)-1H-1,2,4-triazol-3-yl]sulfanyl] acetamide (termed CK37), significantly inhibited choline kinase-α activity and Figure 1a illustrates its potential interaction within the substrate-binding domain of choline kinase-α.

CK37 Inhibits Recombinant Choline Kinase-α

We then used bacterially expressed recombinant human choline kinase-α to assess the effect of CK37 on purified choline kinase enzymatic activity. As illustrated in Figure 1b, CK37 exposure resulted in a dose-dependent suppression of choline kinase-α activity. Since CK37 was identified as a potential competitive inhibitor for the choline binding pocket of choline kinase-α, we examined the competitive effect of choline on the activity of 25μM CK37 against choline kinase-α. We found that increasing the concentration of choline completely reversed the inhibition of choline kinase-α by CK37 (Figure 1c). These data suggest that CK37 is a competitive inhibitor of choline kinase by targeting the choline binding site. To our knowledge, this is the first choline kinase competitive inhibitor that has been identified through *in silico* molecular modeling of the choline binding site within the enzyme.

CK37 Decreases Endogenous Choline Kinase Activity and the Steady-State Concentration of Downstream Choline Metabolites

To investigate the capacity of CK37 to suppress choline kinase activity in whole cells, HeLa cells were incubated with several concentrations of CK37 in the presence of ^{14}C-labeled

choline. As shown in Figure 2a, CK37 inhibited endogenous choline kinase activity at 1μM and had the greatest effect at 10μM (61.7% ± 9.7%). Interestingly, choline uptake was suppressed in the presence of CK37 suggesting that decreased flux through choline kinase may limit the upstream transport of choline. In support of this interpretation, we also observed decreased choline uptake and phosphocholine production in HeLa cells that had been transfected with α-choline kinase-α siRNA that we have previously characterized (Yalcin *et al.*, 2009) (Figure 2b). Together, these results support the conclusion that CK37 inhibits choline kinase-α and the putative role that choline kinase-α may play in regulating choline uptake. We next analyzed the steady-state concentration of phosphocholine by 1D-NMR in HeLa cells treated with 10μM and 50μM CK37. As illustrated in Figure 2c, CK37 caused a dose-dependent decrease in the phosphocholine concentration in as little as one hour. We postulated that decreased phosphocholine production via inhibition of choline kinase-α would result in a decrease in the steady-state concentration of downstream choline metabolites. Lipids from HeLa cells that had been treated with 10μM or 50μM CK37 for 12 hours were methanol extracted and analyzed by ion mass spectrometry. The concentrations of phosphatidylcholine and the potent second messenger phosphatidic acid were reduced by CK37 after twelve hours (Figure 2d). Together, these data suggest that CK37 is able to suppress intracellular choline kinase activity and cause a reduction in the steady-state concentration of both plasma membrane and second messenger phospholipids.

CK37 Attenuates MAPK and PI3K/AKT Signaling

Phosphatidic acid is a downstream product of the Kennedy pathway, which is initiated by the phosphorylation of choline by choline kinase. Phosphatidic acid has been found to be required for the recruitment of a specific Ras guanine-nucleotide exchange factor, Sos, as well as Raf-1 to the plasma membrane (Rizzo *et al.*, 1999; Zhao *et al.*, 2007). In a recent study, we found that selective inhibition of choline kinase-α expression reduced phosphatidic acid and disrupted downstream MAPK and PI3K/AKT signaling (Yalcin *et al.*, 2009). Given that CK37 reduced intracellular phosphatidic acid, we postulated that this compound also may disrupt signaling through MAPK and PI3K/AKT. As shown in Figure 3(a&b), exposure to 10μM CK37 for 12 hours decreased activating phosphorylations of ERK1/2 and AKT, whereas total ERK1/2 and AKT levels remained unchanged. Importantly, viability and cell number at this early time-point were identical between the vehicle control and CK37 exposure groups (*data not shown*).

CK37 Disrupts the Actin Cytoskeleton and Membrane Ruffling

Phosphatidic acid has also been observed to stimulate actin polymerization, and these actin stress fibers have been demonstrated to be required for prolonged MEK activation (Ha and Exton, 1993; Roovers and Assoian, 2003). To investigate cytoskeletal arrangement in response to CK37 treatment, we performed immunofluorescence microscopy on HeLa cells using the small molecule phalloidin, which specifically binds to polymerized F-actin, and an antibody for the focal adhesion protein vinculin. We found that, in the absence of CK37, HeLa cells displayed extensive polymerization of F-actin, which is directly anchored to the membrane at vinculin containing focal adhesion points (Figure 4a, see Vehicle). However, incubation with 10μM CK37 disrupted the localization of focal adhesion points as well as the appearance of actin stress fibers (Figure 4a). Since CK37 altered the cytoskeletal

organization and was found to decrease the main lipid component of the cellular lipid bilayer, phosphatidylcholine, we investigated the effects of CK37 on the plasma membrane. Electron microscopy revealed substantial membrane extensions and ruffling in both HeLa (Figure 4b, see Vehicle) and MDA-MB-231 cells (*data not shown*). However, incubation with 10μM CK37 markedly attenuated these membrane structures, as evident in Figure 4b. Transfection with the choline kinase-α siRNA caused a similar disruption of the actin cytoskeleton and membrane ruffling as observed after CK37 exposure (Figure 4a&b). These data support the conclusion that the structural changes caused by CK37 may be directly related to the inhibition of choline kinase-α activity caused by CK37.

CK37 Selectively Reduces Cancer Cell Proliferation By Targeting Choline Kinase

We examined the sensitivity of six neoplastic cell lines from both solid and hematologic origins to CK37 and found that incubation with CK37 caused a dose-dependent suppression of cell growth in all six tumor cell lines (Figure 5a; IC_{50} values: 5 - 10μM; 48 hours). We next transiently transfected HeLa cells with a plasmid encoding the choline kinase-α open reading frame and examined the effects on the cytostatic activity of CK37. As demonstrated in Figure 5b, over-expression of choline kinase-α conferred resistance to the effects of CK37 compared to vector control cells (IC_{50}: Vector, 4.3μM; +CK, 52μM). These results demonstrate that the cytostatic activity of CK37 is dependent on the level of choline kinase-α expression. We then compared the sensitivity of MDA-MB-231 mammary carcinoma cells, which have an activating mutation of K-ras (von Lintig *et al.*, 2000) to normal untransformed mammary epithelial cells (HMEC). The transformed MDA-MB-231 cells were >5-fold more sensitive to CK37 than the HMECs (compare 50μM HMEC *vs.* 10μM MDA-MB-231, Figure 5c).

Anchorage-independent growth is a hallmark for tumorigenicity of neoplastic cells. We examined the ability of CK37 to suppress HeLa anchorage independent growth in soft agar. CK37 attenuated HeLa soft agar colony formation at 5μM by 86% (Figure 5d&e: Control, 2506 ± 158; +5μM CK37, 360 ± 77). This concentration is below that which is necessary for comparable effects on cell proliferation (>10μM) suggesting that anchorage-independent growth may be especially sensitive to choline kinase-α inhibition.

CK37 Treatment Suppresses *In Vivo* Tumor Growth, Phosphocholine Production, and Activating Phosphorylations of ERK and AKT

In order to define a non-toxic dose of CK37 for use *in vivo*, we intraperitoneally injected C57Bl/6 mice with 0.06, 0.07, and 0.08 mg/g of CK37. We observed no clinical signs of distress at any of the three doses. C57Bl/6 mice bearing Lewis Lung Carcinoma (LLC) xenografts (mean baseline mass = 143 ± 14 mg) were given intraperitoneal injections of 0.08 mg/g CK37 daily for eight days. As shown in Figure 6a, CK37 administration suppressed established tumor growth by 48% compared to the vehicle control group (Vehicle, 1039.6 ± 60.5; + CK37 566.2 ± 67.1). We then measured phosphocholine levels in tumors from both vehicle or treated animals, and found that CK37 administration caused a 51% reduction in tumor phosphocholine compared to tumors from control animals (Figure 6b: Vehicle, 0.027 ± 0.005; + CK37, 0.0145 ± 0.001). Our *in vitro* analysis revealed suppression in the MAPK and AKT pathways upon CK37 treatment, and we and others have

established that choline kinase-α is required for the activation of MAPK and AKT signaling (Chua *et al.*, 2009; Yalcin *et al.*, 2009). We confirmed that LLC ERK and AKT activation was suppressed by CK37 *in vitro* as demonstrated in HeLa cells (*data not shown*). We then performed immunohistochemistry for activating phosphorylations of both ERK (T202/Y204) and AKT (S473) on LLC tumors from vehicle and CK37 treated animals. We observed a marked decrease in the activation of ERK and AKT in tumors extracted from CK37-treated mice (Figure 6c). Quantitative analysis of phospho-ERK and phospho-AKT revealed a decrease in positive cells of 43% and 50%, respectively, in CK37 treated tumors (Figure 6 d&e). Together, these data suggest that CK37 mediated suppression of tumor growth may be due in part to disruption of survival signaling.

Discussion

Metabolomic analyses of human adenocarcinomas have identified a 10-20 fold increase in the steady-state concentration of phosphocholine relative to adjacent normal tissues (Ackerstaff *et al.*, 2003; Degani *et al.*, 1986; Eliyahu *et al.*, 2007; Glunde and Bhujwalla, 2007; Onodera *et al.*, 1986). The high concentration of phosphocholine observed in neoplastic tissues is due in large part to the growth factor activated Ras and PI3K signaling cascades which stimulate choline kinase via the Rho GTPases (Ramirez de Molina *et al.*, 2005; Ramirez de Molina *et al.*, 2002b; Ramirez de Molina *et al.*, 2004b). Phosphocholine serves as an essential metabolic reservoir for the production of phosphatidylcholine, the major phospholipid constituent of membranes and substrate for the production of lipid second messengers (Aoyama *et al.*, 2004; Kent, 1995). In particular, phosphatidic acid, generated from the cleavage of phosphatidylcholine by the Ras and PI3K target phospholipase D2 (Buchanan *et al.*, 2005), has emerged as a key upstream and downstream activator of Ras signaling (Foster and Xu, 2003; Hancock, 2007; Rizzo and Romero, 2002). Phosphatidic acid activates and amplifies Ras signaling by: (i) recruiting the guanine nucleotide-exchange factor Sos (Zhao *et al.*, 2007) and the serine/threonine kinase Raf-1 to the plasma membrane (Rizzo *et al.*, 1999; Rizzo *et al.*, 2000); (ii) stimulating endosome formation necessary for MAP kinase activation (Rizzo and Romero, 2002); and (iii) activating the mammalian target of rapamycin (mTOR) kinase (Fang *et al.*, 2001; Toschi *et al.*, 2008). Taken together, these studies suggest that phosphocholine may be an essential metabolic hub not only for membrane phospholipid synthesis but also for the amplification of neoplastic signaling cascades required for survival and growth.

In a previous study, we demonstrated that the steady-state concentration of phosphocholine is increased in H-Ras^{V12}-transformed human epithelial cells relative to normal human epithelial cells (Yalcin *et al.*, 2009). We then found that siRNA silencing of choline kinase expression in HeLa cells abrogated the high concentration of phosphocholine, which in turn decreased phosphatidic acid and signaling through both the MAPK and PI3K/AKT pathways. This simultaneous reduction in survival signaling resulted in a marked decrease in the anchorage-independent survival of HeLa cells in soft agar and athymic mice. Importantly, combination therapies targeting both PI3K/AKT and MAPK signaling pathways may be a more effective strategy than single pathway disruption in patients with advanced cancers (Kinkade *et al.*, 2008; McCubrey *et al.*, 2007; Salmena *et al.*, 2008). Given that selective inhibition of choline kinase disrupted both pathways, we expected that

small molecule antagonists of choline kinase may have activity against a broad range of human cancers propagated by a diverse combination of signaling pathway mutations.

In the current study, we conducted a computational screen for small molecule inhibitors of choline kinase using the recently solved crystal structure of choline kinase (bound phosphocholine was used for the ligand-based protomol generation). We identified a lead compound that (i) inhibits choline kinase activity and the steady-state concentration of phosphocholine in transformed cells; (ii) is selectively cytotoxic to transformed epithelial cells relative to normal epithelial cells; (iii) decreases ERK and AKT-activating phosphorylations; and (iv) suppresses the growth of xenografts *in vivo*. These studies indicate that *in silico* screening of available compound databases has great utility for the identification of small molecule antagonists of metabolic enzymes.

Neoplastic cells have a substantial need for membrane phospholipids as a result of both rapid cell proliferation and an increased rate of endosome formation required for growth factor signaling (Li *et al.*, 1997; Vieira *et al.*, 1996) and the secretion of microvesicles or exosomes (Iero *et al.*, 2008). For example, cancer cell derived vesicular organelles are elevated in the plasma, ascites and pleural effusions of cancer patients and are believed to be involved in cell-cell communication and immune suppression (Iero *et al.*, 2008). As a result of such high endosome formation and exosome secretion, we anticipate that neoplastic cells require enhanced *de novo* phospholipid synthesis relative to normal cells. The observation that CK37 reduced the steady-state concentration of phosphatidylcholine, plasma membrane ruffling and tumorigenic growth indicates that disruption of *de novo* phospholipid synthesis may be an effective anti-tumor strategy.

The specter of high toxicity caused by pharmacological targeting of choline kinase was recently raised by the observation that homozygous genomic deletion of choline kinase-α causes early embryonic lethality (Wu *et al.*, 2008). However, heterozygous choline kinase knockout mice develop normally without pathology despite decreased choline kinase expression and intracellular phosphocholine in the liver (Wu *et al.*, 2008), suggesting that untransformed wild-type cells may be able to tolerate a large reduction in choline kinase activity *in vivo*. Our observations that CK37 is selectively toxic to transformed cells, attenuates survival signaling and inhibits tumor growth at a non-toxic dose indicates that small molecule antagonists of choline kinase-α may yield favorable therapeutic indices in phase I trials of advanced cancer patients.

Materials and Methods

Choline Kinase-α Virtual Compound Screening

The human choline kinase-α -2 X-ray structure 2CKQ was used as the target structure. The water molecules were stripped from the structure and the target site was the area surrounding the bound phosphocholine. The phosphocholine molecule was stripped but was used to create a ligand-based protomol, with proto_thresh set at 0.2 and proto_bloat at 1, for Surflex-Dock 2.3 (Jain, 2007). The 2007 ZINC (Irwin and Shoichet, 2005) “all purchasable” library containing 2667437 compounds was used with Surflex-Dock to generate a ranked list of candidates. The 50 highest ranked molecules were identified for purchase and, of these,

16 were commercially purchased and examined for inhibitory effects on choline kinase activity. All computational work and virtual screening was done in the JG Brown Cancer Center Molecular Modeling Facility, University of Louisville.

Cell culture

HeLa cervical adenocarcinoma (CCL2), A549 lung adenocarcinoma (CCL-185), Lewis lung carcinoma (CRL-1642), malignant melanoma (A375: CRL-1619), and MDA-MB-231 breast adenocarcinoma (HTB-26) cells were obtained from American Type Culture Collection (ATCC). These cells were cultured in DMEM (Hyclone) supplemented with 10% fetal bovine serum (Hyclone) and 50μg/mL gentamicin sulfate (Invitrogen). Jurkat leukemia cells (ATCC: TIB-152) were cultured in RPMI (Hyclone) supplemented with 10% fetal bovine serum and 50μg/mL gentamicin sulfate. Human mammary epithelial cells (HMEC: Lonza) were grown in mammary epithelial basal medium (Lonza) supplemented according to manufacturer's protocol. All cell lines were maintained at 5% CO_2 at 37°C.

Recombinant Enzyme and *In vitro* Choline Kinase Activity

Choline kinase-α activity was assayed by recombinant enzyme and in intact HeLa cells using previously described methods (Hernandez-Alcoceba *et al.*, 1997). For recombinant choline kinase-α, assays were performed in kinase assay buffer (100mM Tris-HCl, 100mM $MgCl_2$, 10mM ATP, and 2μM methyl[^{14}C]-choline chloride (50-60μCi, mmol). For substrate competition assays, recombinant enzyme was assayed in the presence of several concentrations of choline chloride with or without 25μM CK37. In each case, reactions were carried out at 37°C for one hour and immediately stopped by addition of TCA to a final concentration of 16%. The TCA soluble fraction was then washed 3× with four volumes of water saturated ethyl ether, and dried under vacuum. Metabolites were separated by thin layer chromatography using 60 Å silica gel plates and a liquid phase consisting of 0.9% NaCl: methanol: ammonium hydroxide (50:70:5; V:V:V). Radioactive images from three separate experiments were resolved by PhosphorImager screening and densitometry was performed using Image Quant software.

For *in vitro* HeLa cell labeling, cells were seeded at 1×10^5 cells / mL and incubated with different concentrations of CK37 for 48 hours. Methyl[^{14}C]-choline chloride was added 24 hours before cell harvest, and cells were extracted and analyzed as described above. Densitometry units were normalized to total protein levels for each sample.

NMR Analysis of Intracelluar Phosphocholine Levels

Cells were extracted with cold TCA as previously described (Fan *et al.*, 2008), lyophilized and redissolved in 0.35 mL D_2O containing 90 mM DSS. NMR spectra were recorded at 20° C, 14.1 T on a Varian Inova spectrometer equipped with an inverse triple resonance cold probe. 1-D ^{1}H spectra were recorded with 256 transients, an acquisition time of 2 sec and a recycle time of 5 sec, and referenced to a known concentration of DSS. Peak areas of the phosphocholine resonance at 3.22 ppm, valine, lactate and threonine methyl resonances and DSS were measured using the Varian VNMR software. Where necessary, small corrections for partial saturation were made as described previously using measured T_1 values (Fan *et al.*, 2008). The concentration of phosphocholine was then estimated from the ratio of its

peak area normalized either to DSS, or to the valine methyl group. Valine (or threonine) is an internal standard whose concentration does not change significantly over time (Fan *et al.*, 2008).

Lipidomic Analysis of Choline Metabolites

Lipidomic analysis was performed as a fee for service by the Kansas Lipidomics Research Center at Kansas State University. Briefly, cell lipids were extracted in methanol, dried under continuous nitrogen, and then sent for analysis. The Kansas Lipidomics Research Center Analytical Laboratory is supported from the National Science Foundation's EPSCoR program, under grant no. EPS-0236913 with matching support from the State of Kansas through Kansas Technology Enterprise Corporation and Kansas State University.

ERK1/2 and AKT Phosphorylation

HeLa cells were treated in the absence or presence of several concentrations of CK37 for the indicated time points. Protein extraction and Western blotting was performed as described previously (Telang *et al.*, 2006). Blots were probed for p-ERK1/2 (T202/Y204), p-AKT (S473), total ERK1/2, and total AKT (Cell Signaling, Danvers MA). Densitometry of immunoreactive bands was performed using Quantity One software to calculate the ratio of phosphoprotein / total protein of each target protein.

siRNA Transfection, Actin/Cytoskeleton and Focal Adhesion Immunofluorescence

HeLa cells were grown on slide coverslips and treated in the absence or presence of 10μM CK37 for 48 hours. siRNA transfections were performed as previously described using Lipofectamine RNAiMAX transfection reagent (Invitrogen) following the manufacturer's instructions (Yalcin *et al.*, 2009). The final siRNA concentration was 30nM, and the following siRNA specific for choline kinase-α was used: 5′-GACUGUGGUCCAUUGUACAA-GCCAA-3′ (Invitrogen #CHKAHSS140690). Staining of the actin cytoskeleton and focal adhesion points was performed following the manufacturer's protocol (Millipore). Briefly, cells were fixed with 4% paraformaldehyde and permeabilized with addition of 0.1% Triton X. The vinculin focal adhesion protein was visualized using α-vinculin antibody followed by α-rat AlexaFluor 488 secondary antibody. F-actin was assayed by addition of TRITC-conjugated phalloidin. Immunofluorescence images were generated using the Olympus BX51WI confocal microscope with Fluoview software.

Electron Microscopy

HeLa cells were treated in the absence or presence of 10μM CK37 for 48 hours. siRNA transfections were performed as described above. In both scenarios, samples were fixed in cacodylate buffered 3% glutaraldehyde for 16 hours at 4°C. They were subsequently postfixed in cacodylate-buffered 1% osmium tetroxide for one hour, dehydrated through a series of graded alcohols, and embedded in LX-112 epoxy plastic (Ladd Research Industries). 80 μM sections were cut on a LKB 8800 ultratone utilizing a diamond knife, mounted on 200 mesh copper grids, stained with uranium acetate and lead citrate, and viewed with a Phelps CM 12 electron microscope operating at 60KV.

In vitro CK37 Cell Growth Inhibition

All cell lines were plated at 1×10^5/mL in the appropriate medium. For suspension cells, CK37 was added immediately to the medium, whereas CK37 treatment was initiated the following day for adherent cell lines. For the choline kinase-α over-expression experiment, HeLa cells were transiently transfected with vector alone or choline kinase-α expression plasmid (pIRES-neo-CK), and CK37 was added to the medium 48 hours post-transfection. In all cases, cells were collected 48 hours after treatment, and cell number and viability were determined by trypan blue exclusion. The IC_{50} for each experiment was calculated as the CK37 concentration needed for 50% of vehicle-treated cell growth. The data represented are the mean ± STD from triplicate measurements from three independent experiments.

Soft Agar Colony Formation

HeLa cells were plated at a density of 25×10^3 cells per 60-mm plate with 3mL bottom agar (0.6%) and 2mL top agar (0.3%) in normal growth medium. Cells were fed every three days by addition of a new layer of top agar which contained several concentrations of CK37. After 14 days of growth, colonies were counted from random 1cm squared sections of each plate.

In Vivo Study

Exponentially growing Lewis lung carcinoma cells were collected, washed twice, and resuspended in PBS (1×10^7/mL). C57Bl/6 female mice (20 g) were injected s.c. with 0.1 mL of the suspension. Body weight and tumor growth were monitored daily throughout the study. Tumor masses were determined by measurement with Vernier calipers using the formula: mass (mg) = [width^2 (mm) × length (mm)] / 2 (Taetle *et al.*, 1987). Mice with established tumors (between 130 and 190 mg) were randomized into vehicle control or CK37 treated groups. Vehicle control groups received i.p. injections of 50 μL DMSO, whereas treated groups received 0.08 mg/g CK37 in 50 μL DMSO at the indicated time points. All protocols were approved by the University of Louisville Institutional Animal Care and Use Committee. Phosphocholine levels in resected tumors were measured by TCA extraction of frozen tumor sections and subsequent analysis by 1D-NMR as described above. Phosphocholine levels were normalized to the stable metabolite valine and to the dry weight of the TCA extracted tumor section. Immunohistochemical analyses were performed on paraffin embedded tumor sections by IHCtech, LLC (Aurora, CO) using p-AKT (S473) (Novacastra, United Kingdom) and p-ERK (T202/Y204) (PhosphoSolutions, Aurora, CO) as well as the corresponding isotype control antibodies. The intensity of immunoreactive cells in a 400× field image was graded in a blinded fashion as weakly positive (1), moderately positive (2), or strongly positive (3).

Statistics

Statistical significance for choline kinase-α inhibition, growth and soft agar colony formation inhibition, and *in vivo* studies between control and CK37 treatment was determined by a two-sample, nonparametric, two-tailed t-test using Graph Pad Prism version 3.0 (Graph Pad Software). $p < 0.05$ was considered to be statistically significant.

Acknowledgments

We acknowledge Deanna Siow and Binks Wattenburg for assistance with the thin layer chromatography protocol, Erin Brock for assisting with the confocal microscopy experiments, Bennet Jenson for histopathology assistance, and Andrew Lane for NMR interpretation. We also thank Dr. Arnon Lavie for providing the Δ49N- hCKα2 plasmid for the expression of recombinant choline kinase. NMR experiments were carried out at the James Graham Brown Cancer Center NMR facility, supported in part by the Brown Foundation and NCCRR grant 1P20 RR18733. This work was supported by institutional funds from the James Graham Brown Cancer Center and by grants from the Ky Lung Cancer Research Program (JC & BFC) and the National Cancer Institute (JC: 2R56CA116428-0509).

References

Ackerstaff E, Glunde K, Bhujwalla ZM. Choline phospholipid metabolism: a target in cancer cells? J Cell Biochem. 2003; 90:525–33. [PubMed: 14523987]

Aoyama C, Liao H, Ishidate K. Structure and function of choline kinase isoforms in mammalian cells. Prog Lipid Res. 2004; 43:266–81. [PubMed: 15003397]

Buchanan FG, McReynolds M, Couvillon A, Kam Y, Holla VR, Dubois RN, et al. Requirement of phospholipase D1 activity in H-RasV12-induced transformation. Proc Natl Acad Sci U S A. 2005; 102:1638–42. [PubMed: 15668389]

Chua BT, Gallego-Ortega D, Ramirez de Molina A, Ullrich A, Lacal JC, Downward J. Regulation of Akt(ser473) phosphorylation by Choline kinase in breast carcinoma cells. Mol Cancer. 2009; 8:131. [PubMed: 20042122]

Chung T, Huang JS, Mukherjee JJ, Crilly KS, Kiss Z. Expression of human choline kinase in NIH 3T3 fibroblasts increases the mitogenic potential of insulin and insulin-like growth factor I. Cell Signal. 2000; 12:279–88. [PubMed: 10822168]

Degani H, Horowitz A, Itzchak Y. Breast tumors: evaluation with P-31 MR spectroscopy. Radiology. 1986; 161:53–5. [PubMed: 3020609]

Eliyahu G, Kreizman T, Degani H. Phosphocholine as a biomarker of breast cancer: molecular and biochemical studies. Int J Cancer. 2007; 120:1721–30. [PubMed: 17236204]

Exton JH. Signaling through phosphatidylcholine breakdown. J Biol Chem. 1990; 265:1–4. [PubMed: 2104616]

Fan TW, Kucia M, Jankowski K, Higashi RM, Ratajczak J, Ratajczak MZ, et al. Rhabdomyosarcoma cells show an energy producing anabolic metabolic phenotype compared with primary myocytes. Mol Cancer. 2008; 7:79. [PubMed: 18939998]

Fang Y, Vilella-Bach M, Bachmann R, Flanigan A, Chen J. Phosphatidic acid-mediated mitogenic activation of mTOR signaling. Science. 2001; 294:1942–5. [PubMed: 11729323]

Foster DA, Xu L. Phospholipase D in cell proliferation and cancer. Mol Cancer Res. 2003; 1:789–800. [PubMed: 14517341]

Glunde K, Bhujwalla ZM. Choline kinase alpha in cancer prognosis and treatment. Lancet Oncol. 2007; 8:855–7. [PubMed: 17913651]

Glunde K, Raman V, Mori N, Bhujwalla ZM. RNA interference-mediated choline kinase suppression in breast cancer cells induces differentiation and reduces proliferation. Cancer Res. 2005; 65:11034–43. [PubMed: 16322253]

Glunde K, Shah T, Winnard PT Jr, Raman V, Takagi T, Vesuna F, et al. Hypoxia regulates choline kinase expression through hypoxia-inducible factor-1 alpha signaling in a human prostate cancer model. Cancer Res. 2008; 68:172–80. [PubMed: 18172309]

Ha KS, Exton JH. Activation of actin polymerization by phosphatidic acid derived from phosphatidylcholine in IIC9 fibroblasts. J Cell Biol. 1993; 123:1789–96. [PubMed: 8276897]

Hancock JF. PA promoted to manager. Nat Cell Biol. 2007; 9:615–7. [PubMed: 17541412]

Hernandez-Alcoceba R, Fernandez F, Lacal JC. In vivo antitumor activity of choline kinase inhibitors: a novel target for anticancer drug discovery. Cancer Res. 1999; 59:3112–8. [PubMed: 10397253]

Hernandez-Alcoceba R, Saniger L, Campos J, Nunez MC, Khaless F, Gallo MA, et al. Choline kinase inhibitors as a novel approach for antiproliferative drug design. Oncogene. 1997; 15:2289–301. [PubMed: 9393874]

Iero M, Valenti R, Huber V, Filipazzi P, Parmiani G, Fais S, et al. Tumour-released exosomes and their implications in cancer immunity. Cell Death Differ. 2008; 15:80–8. [PubMed: 17932500]

Iorio E, Mezzanzanica D, Alberti P, Spadaro F, Ramoni C, D'Ascenzo S, et al. Alterations of choline phospholipid metabolism in ovarian tumor progression. Cancer Res. 2005; 65:9369–76. [PubMed: 16230400]

Irwin JJ, Shoichet BK. ZINC--a free database of commercially available compounds for virtual screening. J Chem Inf Model. 2005; 45:177–82. [PubMed: 15667143]

Jain AN. Surflex-Dock 2.1: robust performance from ligand energetic modeling, ring flexibility, and knowledge-based search. J Comput Aided Mol Des. 2007; 21:281–306. [PubMed: 17387436]

Jimenez B, del Peso L, Montaner S, Esteve P, Lacal JC. Generation of phosphorylcholine as an essential event in the activation of Raf-1 and MAP-kinases in growth factors-induced mitogenic stimulation. J Cell Biochem. 1995; 57:141–9. [PubMed: 7721953]

Kent C. Eukaryotic phospholipid biosynthesis. Annu Rev Biochem. 1995; 64:315–43. [PubMed: 7574485]

Kinkade CW, Castillo-Martin M, Puzio-Kuter A, Yan J, Foster TH, Gao H, et al. Targeting AKT/mTOR and ERK MAPK signaling inhibits hormone-refractory prostate cancer in a preclinical mouse model. J Clin Invest. 2008; 118:3051–64. [PubMed: 18725989]

Ko KW, Cook HW, Vance DE. Reduction of phosphatidylcholine turnover in a Nb 2 lymphoma cell line after prolactin treatment. A novel mechanism for control of phosphatidylcholine levels in cells. J Biol Chem. 1986; 261:7846–52. [PubMed: 3519613]

Li G, D'Souza-Schorey C, Barbieri MA, Cooper JA, Stahl PD. Uncoupling of membrane ruffling and pinocytosis during Ras signal transduction. J Biol Chem. 1997; 272:10337–40. [PubMed: 9099668]

Malito E, Sekulic N, Too WC, Konrad M, Lavie A. Elucidation of human choline kinase crystal structures in complex with the products ADP or phosphocholine. J Mol Biol. 2006; 364:136–51. [PubMed: 17007874]

McCubrey JA, Steelman LS, Franklin RA, Abrams SL, Chappell WH, Wong EW, et al. Targeting the RAF/MEK/ERK, PI3K/AKT and p53 pathways in hematopoietic drug resistance. Adv Enzyme Regul. 2007; 47:64–103. [PubMed: 17382374]

Neeman M, Degani H. Early estrogen-induced metabolic changes and their inhibition by actinomycin D and cycloheximide in human breast cancer cells: 31P and 13C NMR studies. Proc Natl Acad Sci U S A. 1989; 86:5585–9. [PubMed: 2748604]

Onodera K, Okubo A, Yasumoto K, Suzuki T, Kimura G, Nomoto K. 31P nuclear magnetic resonance analysis of lung cancer: the perchloric acid extract spectrum. Jpn J Cancer Res. 1986; 77:1201–6. [PubMed: 3029002]

Ramirez de Molina A, Banez-Coronel M, Gutierrez R, Rodriguez-Gonzalez A, Olmeda D, Megias D, et al. Choline kinase activation is a critical requirement for the proliferation of primary human mammary epithelial cells and breast tumor progression. Cancer Res. 2004a; 64:6732–9. [PubMed: 15374991]

Ramirez de Molina A, Gallego-Ortega D, Sarmentero J, Banez-Coronel M, Martin-Cantalejo Y, Lacal JC. Choline kinase is a novel oncogene that potentiates RhoA-induced carcinogenesis. Cancer Res. 2005; 65:5647–53. [PubMed: 15994937]

Ramirez de Molina A, Gutierrez R, Ramos MA, Silva JM, Silva J, Bonilla F, et al. Increased choline kinase activity in human breast carcinomas: clinical evidence for a potential novel antitumor strategy. Oncogene. 2002a; 21:4317–22. [PubMed: 12082619]

Ramirez de Molina A, Penalva V, Lucas L, Lacal JC. Regulation of choline kinase activity by Ras proteins involves Ral-GDS and PI3K. Oncogene. 2002b; 21:937–46. [PubMed: 11840339]

Ramirez de Molina A, Rodriguez-Gonzalez A, Gutierrez R, Martinez-Pineiro L, Sanchez J, Bonilla F, et al. Overexpression of choline kinase is a frequent feature in human tumor-derived cell lines and in lung, prostate, and colorectal human cancers. Biochem Biophys Res Commun. 2002c; 296:580–3. [PubMed: 12176020]

Ramirez de Molina A, Rodriguez-Gonzalez A, Lacal JC. From Ras signalling to ChoK inhibitors: a further advance in anticancer drug design. Cancer Lett. 2004b; 206:137–48. [PubMed: 15013519]

Rizzo M, Romero G. Pharmacological importance of phospholipase D and phosphatidic acid in the regulation of the mitogen-activated protein kinase cascade. Pharmacol Ther. 2002; 94:35–50. [PubMed: 12191592]

Rizzo MA, Shome K, Vasudevan C, Stolz DB, Sung TC, Frohman MA, et al. Phospholipase D and its product, phosphatidic acid, mediate agonist-dependent raf-1 translocation to the plasma membrane and the activation of the mitogen-activated protein kinase pathway. J Biol Chem. 1999; 274:1131–9. [PubMed: 9873061]

Rizzo MA, Shome K, Watkins SC, Romero G. The recruitment of Raf-1 to membranes is mediated by direct interaction with phosphatidic acid and is independent of association with Ras. J Biol Chem. 2000; 275:23911–8. [PubMed: 10801816]

Rodriguez-Gonzalez A, Ramirez de Molina A, Fernandez F, Ramos MA, del Carmen Nunez M, Campos J, et al. Inhibition of choline kinase as a specific cytotoxic strategy in oncogene-transformed cells. Oncogene. 2003; 22:8803–12. [PubMed: 14654777]

Roovers K, Assoian RK. Effects of rho kinase and actin stress fibers on sustained extracellular signal-regulated kinase activity and activation of G(1) phase cyclin-dependent kinases. Mol Cell Biol. 2003; 23:4283–94. [PubMed: 12773570]

Salmena L, Carracedo A, Pandolfi PP. Tenets of PTEN tumor suppression. Cell. 2008; 133:403–14. [PubMed: 18455982]

Scales SJ, Scheller RH. Lipid membranes shape up. Nature. 1999; 401:123–4. [PubMed: 10490016]

Taetle R, Rosen F, Abramson I, Venditti J, Howell S. Use of nude mouse xenografts as preclinical drug screens: in vivo activity of established chemotherapeutic agents against melanoma and ovarian carcinoma xenografts. Cancer Treat Rep. 1987; 71:297–304. [PubMed: 3815395]

Telang S, Yalcin A, Clem AL, Bucala R, Lane AN, Eaton JW, et al. Ras transformation requires metabolic control by 6-phosphofructo-2-kinase. Oncogene. 2006; 25:7225–34. [PubMed: 16715124]

Toschi A, Lee E, Xu L, Garcia A, Gadir N, Foster DA. Regulation of mTORC1 and mTORC2 Complex Assembly by Phosphatidic Acid - a Competition with Rapamycin. Mol Cell Biol. 2008

Uchida T. Stimulation of phospholipid synthesis in HeLa cells by epidermal growth factor and insulin: activation of choline kinase and glycerophosphate acyltransferase. Biochim Biophys Acta. 1996; 1304:89–104. [PubMed: 8954133]

Vieira AV, Lamaze C, Schmid SL. Control of EGF receptor signaling by clathrin-mediated endocytosis. Science. 1996; 274:2086–9. [PubMed: 8953040]

von Lintig FC, Dreilinger AD, Varki NM, Wallace AM, Casteel DE, Boss GR. Ras activation in human breast cancer. Breast Cancer Res Treat. 2000; 62:51–62. [PubMed: 10989985]

Warden CH, Friedkin M. Regulation of choline kinase activity and phosphatidylcholine biosynthesis by mitogenic growth factors in 3T3 fibroblasts. J Biol Chem. 1985; 260:6006–11. [PubMed: 2987212]

Wu G, Aoyama C, Young SG, Vance DE. Early embryonic lethality caused by disruption of the gene for choline kinase alpha, the first enzyme in phosphatidylcholine biosynthesis. J Biol Chem. 2008; 283:1456–62. [PubMed: 18029352]

Yalcin A, Clem B, Makoni S, Clem A, Nelson K, Thornburg J, et al. Selective inhibition of choline kinase simultaneously attenuates MAPK and PI3K/AKT signaling. Oncogene. 2009; 29:139–49. [PubMed: 19855431]

Zhao C, Du G, Skowronek K, Frohman MA, Bar-Sagi D. Phospholipase D2-generated phosphatidic acid couples EGFR stimulation to Ras activation by Sos. Nat Cell Biol. 2007; 9:706–12. [PubMed: 17486115]

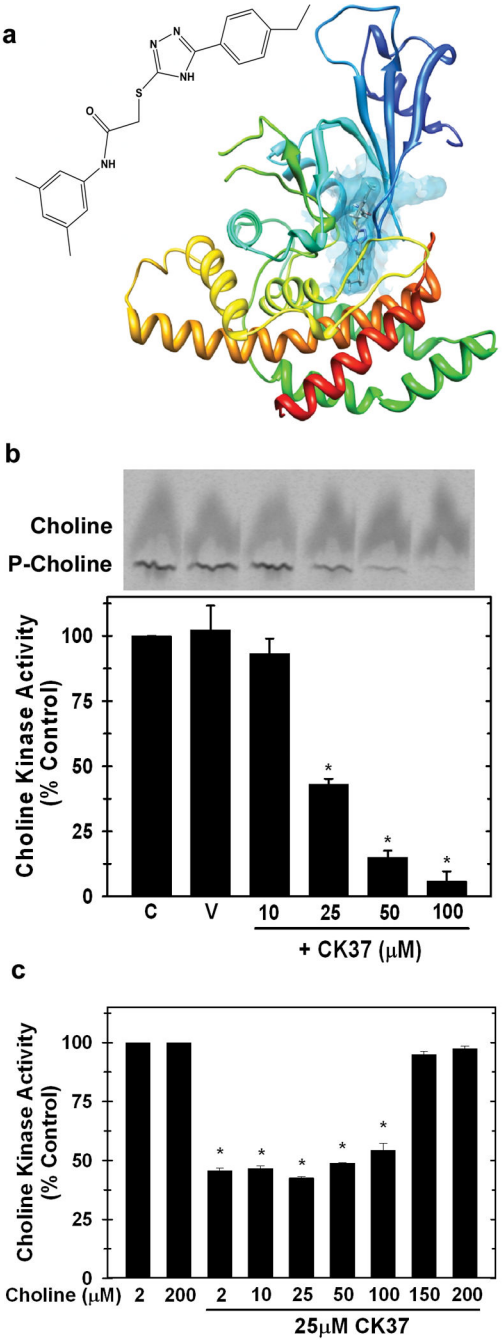

Figure 1. Computational identification of a novel small molecule inhibitor of choline kinase-α, CK37

a. Molecular structure of CK37 and the secondary structure of choline kinase-α with CK37 (rod) depicted within the active site of the protein. **b.** Recombinant choline kinase activity assays were performed with 2μM ^{14}C-choline chloride in the presence of 10, 25, 50, and 100μM CK37. Representative thin layer chromatography (t.l.c.) plate examining choline and phosphocholine levels with several concentrations of CK37. Data are represented as % of control activity for each CK37 concentration. Mean ± STD of three independent experiments. $p < 0.05$. **c.** Recombinant choline kinase activity assays were performed with

different total choline concentrations (2, 10, 25, 50, 100, 150, and 200μM) in the presence or absence of 25μM CK37. Data are represented as % of control activity for each concentration of choline, and shown are mean ± STD from two separate experiments. $p < 0.05$.

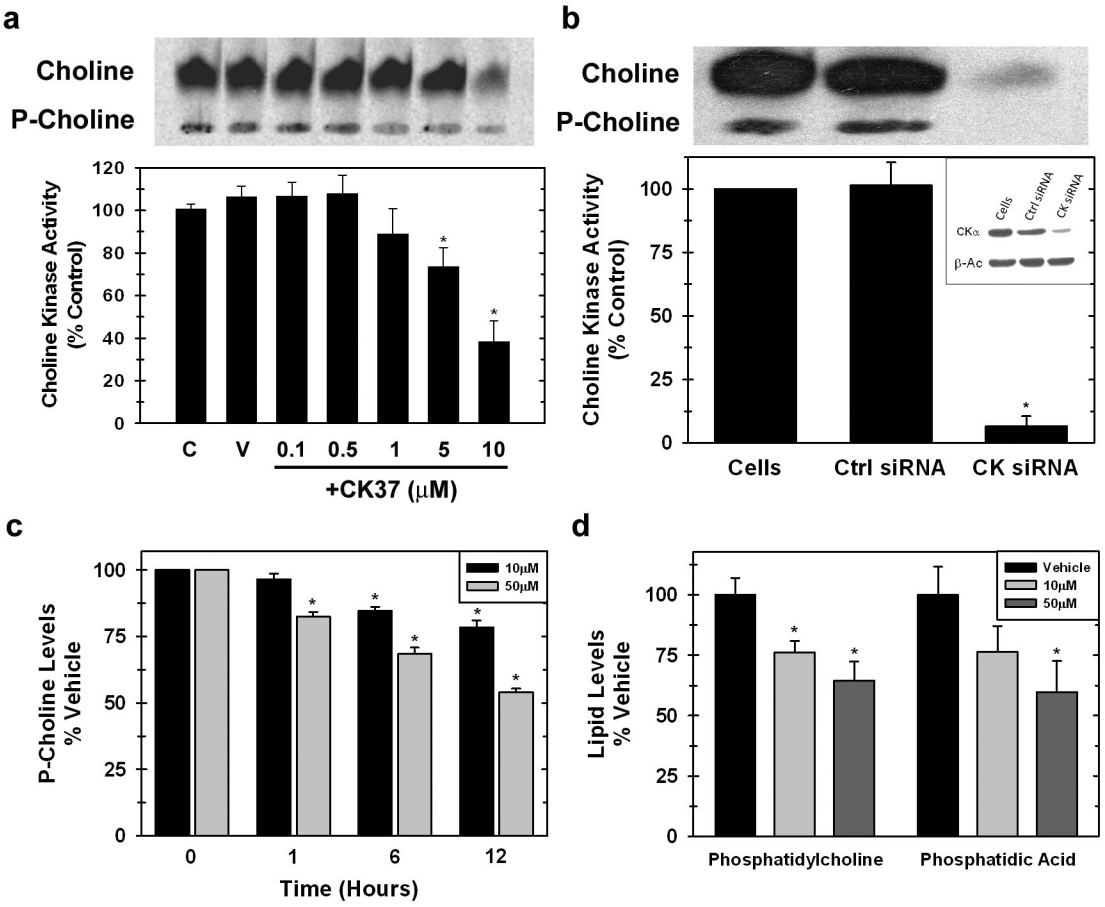

Figure 2. CK37 exposure inhibits endogenous choline kinase-α activity and decreases levels of downstream choline metabolites

Hela cells were labeled with ^{14}C-choline chloride treated with or without **(a)** several concentrations of CK37 or **(b)** siRNA silencing of choline kinase-α, and metabolites were analyzed by thin layer chromatography (t.l.c.). Shown is a representative t.l.c. plate examining choline and P-choline levels. Data are represented as % of control activity and mean ± STD of three independent experiments. $p < 0.05$. **c.** Intracellular phosphocholine levels from HeLa cells treated with vehicle or several concentrations of CK37 for 1, 6, or 12 hours were analyzed by 1-D NMR spectrometry. **d.** Phosphatidylcholine and phosphatidic acid levels were determined by lipidomic analysis from methanol extracted lipids from HeLa cells treated with different concentrations of CK37 for 12 hours.

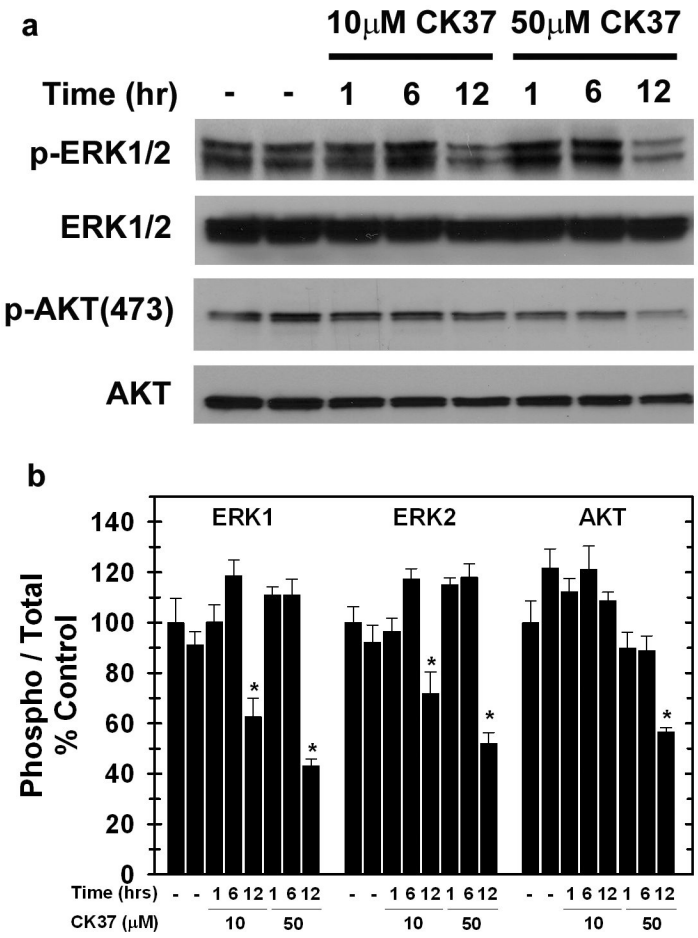

Figure 3. CK37 decreases activating phosphorylations of ERK and AKT

a. Analysis of ERK1/2 and AKT activation in the presence of CK37 was performed by Western blot analysis. Representative immunoblot depicting p-ERK1/2 (T202/Y204), ERK1/2, p-AKT (S473), and AKT levels from two independent experiments. **b.** Densitometry analysis was performed to determine the phospho / total ratio for AKT, ERK1, and ERK2.

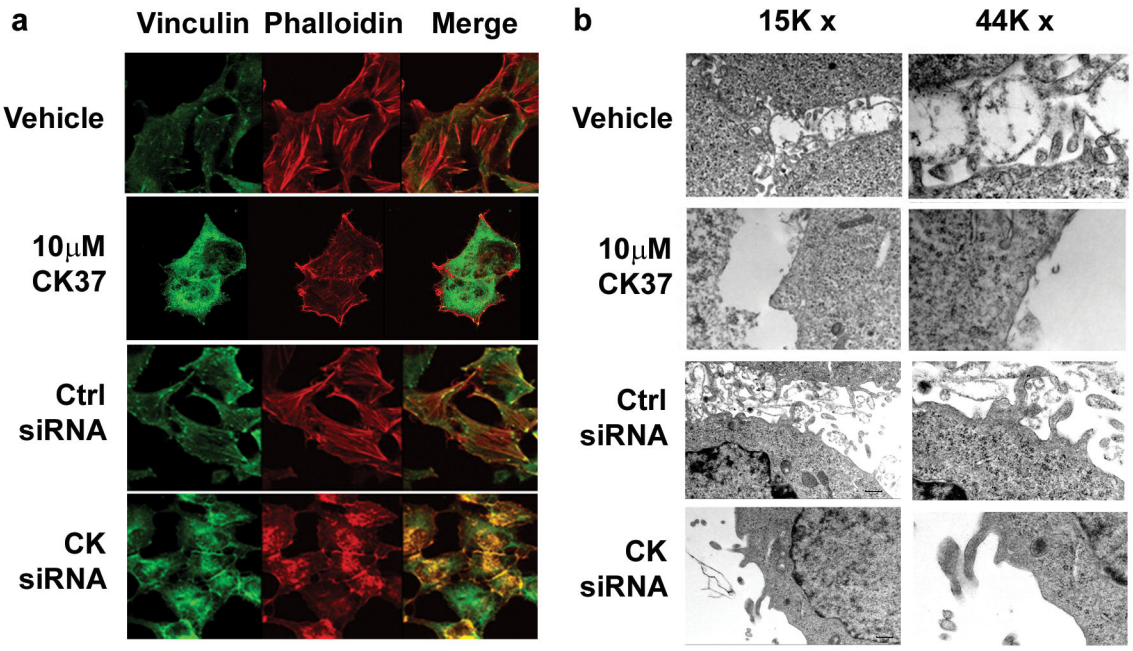

Figure 4. Inhibition of choline kinase by CK37 or specific siRNA silencing disrupts the actin cytoskeleton and causes ultrastructural changes in the plasma membrane

a. Immunofluorescence confocal microscopy was performed to analyze the effect of CK37 or siRNA silencing on the actin cytoskeleton arrangement in HeLa cells. Representative images for vinculin, phalloidin and merged staining from vehicle or 10μM CK37 treated cells or cells that were either transfected with scrambled control (Ctrl siRNA) or choline kinase-α specific siRNA (CK siRNA) for 48 hrs. **b.** Electron microscopy was performed to evaluate the membrane structure of HeLa cells in the presence of CK37 or choline kinase-specific siRNA. Represented are HeLa cell electron micrographs at 15000× and 44000× magnification from vehicle or 10μM CK37 treated samples, or cells that were either transfected with scrambled control (Ctrl siRNA) or choline kinase-α specific siRNA (CK siRNA) for 48 hrs.

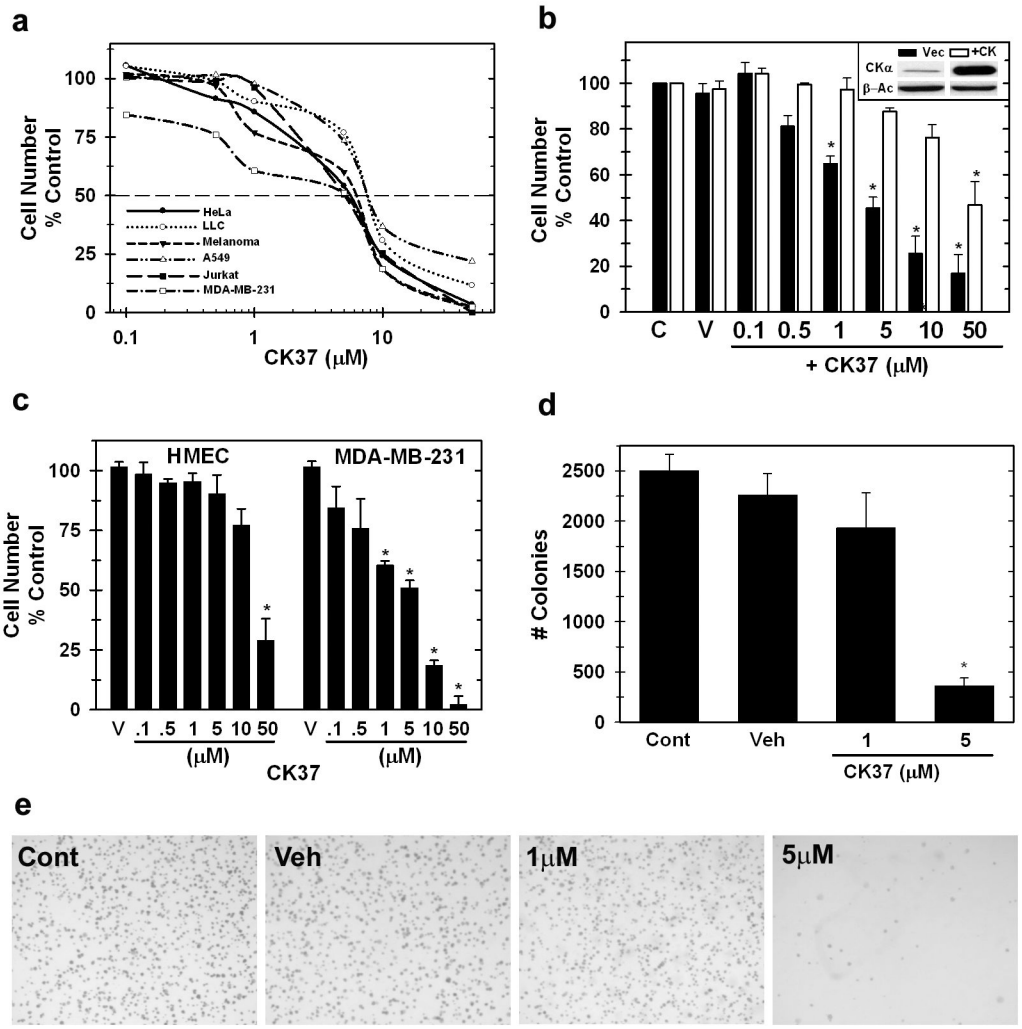

Figure 5. CK37 selectively suppresses tumor cell proliferation and anchorage-independent growth

a. Cell proliferation assays were performed after 48 hours of treatment with or without CK37. Data are represented as % of cell growth of vehicle control as $\log_{10}$ of CK37 from duplicate values in three independent experiments. **b.** Target specificity of CK37 is demonstrated by the loss of CK37 suppression of HeLa cell proliferation by over-expression of choline kinase-α. Data is represented as % of cell growth of vehicle control of each cell line for each concentration of CK37 from duplicate values from three independent experiments. $p < 0.05$. **c.** Anti-proliferation assays were performed on MDA-MB-231 breast tumor cells compared to primary human mammary epithelial cells (HMEC) to analyze the selective inhibition of CK37 for transformed versus normal cells. **d.** Densitometry analysis of soft-agar colony formation between different CK37 treated samples. Colonies from three separate one cm^2 boxes per plate were enumerated, and shown are mean ± STD colonies from two different experiments. * $p < 0.5$. **e.** Anchorage-independent growth of HeLa cells treated with several concentrations of CK37 was assessed by colony formation in soft agar. Shown are representative images from control, vehicle, 1μM CK37, or 5μM CK37 treated soft-agar plates from two separate experiments.

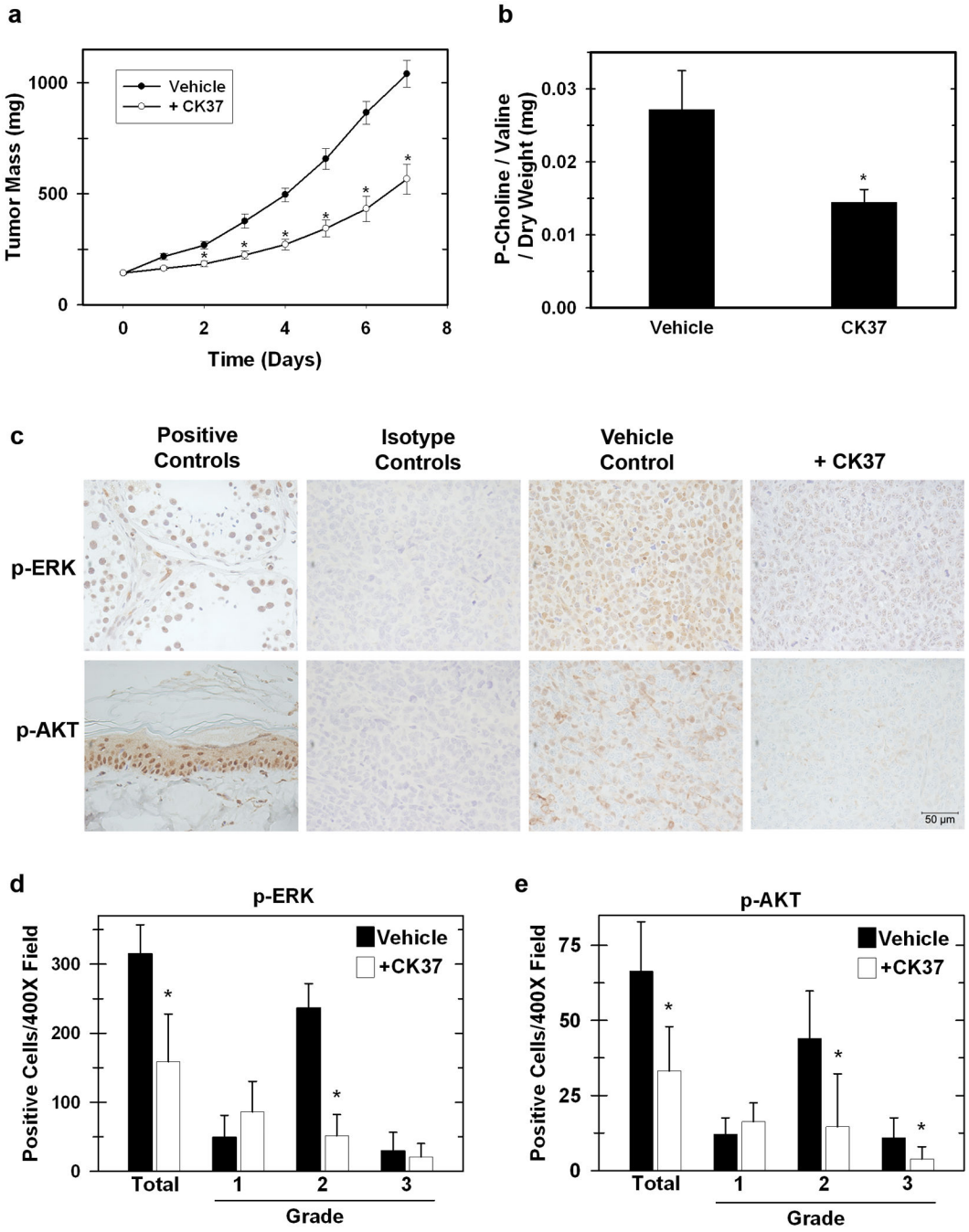

Figure 6. Intraperitoneal administration of CK37 suppresses tumor growth, phosphocholine levels, and activating phosphorylations of ERK and AKT *in vivo*

a. Tumors were measured daily using blunt-end Vernier calipers, and mice with established tumors were blindly randomized into either Vehicle (filled circles) or CK37 treatment (open circles) groups. Mice were administered daily intraperitoneal doses of either 50 µL DMSO (n=10) or 0.08 mg / g of CK37 (n=10) in 50 µL DMSO at the indicated time points. Data are presented as mean ± SEM. A significant difference ($p < 0.01$) was observed at day 2 of administration. **b.** Phosphocholine was measured in resected tumors by 1D-NMR analysis.

Phosphocholine levels were normalized to the stable metabolite valine and to dry weight of the extracted tumor section. * $p < 0.5$ **c.** Tumors from vehicle or CK37 treated groups were analyzed by immunohistochemistry for p-ERK (T202/Y204) and p-AKT (S473). Shown are representative 400× field images of tumor sections from vehicle and CK37 treated groups as well as the corresponding isotype controls. Positive controls: phospho-ERK – testes, phospho-AKT – rat tail skin. **d&e.** Positive cells from three 400× image fields were quantified from three different tumors for both DMSO and CK37 treated groups. Shown is the mean expression score of p-ERK and p-AKT protein. The intensity of the immunoreactivity was graded as weakly positive (1), moderately positive (2), or strongly positive (3). * $p < 0.5$.